

Bloch surface waves-controlled emission of organic dyes grafted on a one-dimensional photonic crystal

Mirko Ballarini, Francesca Frascella, Francesco Michelotti, Gabriella Digregorio, Paola Rivolo et al.

Citation: *Appl. Phys. Lett.* **99**, 043302 (2011); doi: 10.1063/1.3616144

View online: <http://dx.doi.org/10.1063/1.3616144>

View Table of Contents: <http://apl.aip.org/resource/1/APPLAB/v99/i4>

Published by the [American Institute of Physics](#).

Related Articles

Fractal phononic crystals in aluminum nitride: An approach to ultra high frequency bandgaps
Appl. Phys. Lett. **99**, 163501 (2011)

Independent electrical tuning of separated quantum dots in coupled photonic crystal cavities
Appl. Phys. Lett. **99**, 161102 (2011)

Electron and hole scattering in short-period InGaAs/InP superlattices
J. Appl. Phys. **110**, 073706 (2011)

Transmission of terahertz wave through one-dimensional photonic crystals containing single and multiple metallic defects
J. Appl. Phys. **110**, 073101 (2011)

Temperature dependent resonances in superconductor photonic crystal
J. Appl. Phys. **110**, 063513 (2011)

Additional information on *Appl. Phys. Lett.*

Journal Homepage: <http://apl.aip.org/>

Journal Information: http://apl.aip.org/about/about_the_journal

Top downloads: http://apl.aip.org/features/most_downloaded

Information for Authors: <http://apl.aip.org/authors>

ADVERTISEMENT

**AIP**Advances

Submit Now

**Explore AIP's new
open-access journal**

- **Article-level metrics
now available**
- **Join the conversation!
Rate & comment on articles**

Bloch surface waves-controlled emission of organic dyes grafted on a one-dimensional photonic crystal

Mirko Ballarini,^{1,a)} Francesca Frascella,² Francesco Michelotti,³ Gabriella Digregorio,² Paola Rivolo,² Vincent Paeder,⁴ Valeria Musi,⁴ Fabrizio Giorgis,¹ and Emiliano Descrovi²

¹Dipartimento di Fisica, Politecnico di Torino, C.so Duca degli Abruzzi 24, 10129 Torino, Italy

²Dipartimento di Scienza dei Materiali e Ingegneria Chimica, Politecnico di Torino, C.so Duca degli Abruzzi 24, 10129 Torino, Italy

³Dipartimento di Scienze di Base e Applicate per l'Ingegneria, SAPIENZA Università di Roma, Via A. Scarpa, 16 00161 Roma, Italy

⁴Optics and Photonics Technology Laboratory, Ecole Polytechnique Fédérale de Lausanne (EPFL), Breguet 2, 2000 Neuchâtel, Switzerland

(Received 27 May 2011; accepted 7 July 2011; published online 27 July 2011)

An alternative route to plasmon-controlled fluorescence for improving the detection of fluorescence is proposed. In place of a metallic layer, a suitable silicon-based one-dimensional photonic crystal is used to generate a Bloch surface waves-coupled emission from a thin polymeric layer decorated with a fluorescent dye. Fluorescent radiation coupled to Bloch surface waves is strongly polarized and directional, with an angular divergence of 0.3° corresponding to a spectral bandwidth of 3 nm. Within this range, an overall signal enhancement of a factor larger than 500 is obtained as compared to a conventional glass substrate thanks to an additional enhancement mechanism based on dyes excitation via Bloch surface waves. © 2011 American Institute of Physics. [doi:10.1063/1.3616144]

The use of surface plasmon polaritons (SPPs) for the modification of the emission properties of a fluorophore in close proximity of a metal surface has been well documented.¹ Mainly two SPP-based techniques have emerged for controlling the enhancement, polarization, and direction of the emitted fluorescence, namely, the surface plasmon field-enhanced fluorescence (SPFS) and the surface plasmon-coupled fluorescence (SPCE).^{2,3} In the SPFS, one benefits from the enhanced excitation of the emitters upon a resonant coupling of the illuminating (laser) radiation to the SPP sustained by the metallic film, leading to an overall measured enhanced fluorescence.⁴ Conversely, SPCE is based on the coupling of fluorescence into the SP mode of the metal film, which is re-irradiated only at angles that satisfy the SPR dispersion relation.⁵ In particular, this latter method has been proposed as a tool to significantly improve the detection performances.⁶ SPCE is most useful for the strong directionality of fluorescence emission, which results in a higher signal-to-noise ratio, and for applications where multiplexing is desired.⁷ However, a deeper theoretical study has shown that the advantage of SPCE with respect to the enhanced fluorescence signal is strongly mitigated by the attenuation of the detectable signal through the metal layer, making this technique comparable to others that are not based on SPR.⁸ It is also well known that SPCE and SPFE are highly dependent on the distance between the metal/dielectric interface and the position of the emitter.⁹

We propose an alternative method for the detection of the enhanced fluorescence based on Bloch surface waves (BSWs) propagating at the truncation surface of a finite one dimensional photonic crystal (1DPC). The benefits over the above mentioned techniques is twofold. Firstly, BSW-based

detection does not suffer from signal losses, being the enhancing medium made of dielectrics. Secondly, the distance between the emitters and the 1DPC surface is less critical due to the absence of quenching and strong absorption effects played by metals.

BSWs, which may be considered the dielectric analogue of the SPPs, have been recently proposed for a variety of sensing applications, including label-free bio- and gas-sensing.^{10,11}

Here, we consider a 1DPC made of a high index material H (silicon nitride, $n_H = 1.99$ at $\lambda = 532.0$ nm) and low-index material L (silicon dioxide, $n_L = 1.48$ at $\lambda = 532.0$ nm) grown by plasma enhanced chemical vapour deposition (Oxford Plasmalab 80+ PECVD) and arranged in 15 layers as follows: glass/(HL)⁷L1/air. Each layer in the periodic stack has a respective thickness $t_H = 79$ nm, $t_L = 134$ nm, while the last tailoring layer at the air side has a thickness $t_{L1} = 28$ nm. On the top of the 1DPC, a 30 nm thin polymeric layer ($n = 1.53$) has been obtained by plasma polymerization deposition of acrylic acid (PPAA).¹² PPAA can expose up to 10^{16} -COOH functional groups/cm² suitable for protein binding. Subsequently, a solution containing protein A labelled with Alexa Fluor 546 has been incubated at concentration 0.1 mg/ml for 30 min on the polymeric layer. After washing, a 1DPC with a homogeneously fluorescent polymeric cap is obtained.

The fabricated structure sustains BSWs according to Fig. 1(a), where the reflectance map $R(\lambda, \theta_e)$ is calculated as a function of wavelength and excitation angle θ_e . The BSW dispersion appears as a narrow low-reflectivity region beyond the air light line. At $\lambda = 532.0$ nm, a BSW is coupled at $\theta_e = 49.1^\circ$. In the calculation of $R(\lambda, \theta_e)$, the absorption from the dye was not taken into account; therefore, the width of the resonances depends only on the intrinsic absorption coefficients of the materials in the stack.

^{a)}Author to whom correspondence should be addressed. Electronic mail: mirko.ballarini@polito.it.

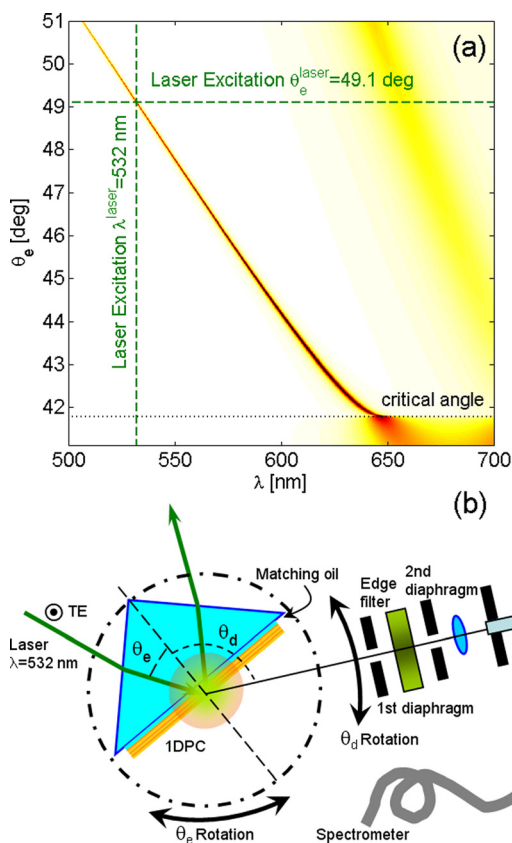


FIG. 1. (Color online) (a) Calculated reflectance map $R(\lambda, \theta_e)$ for a 1DPC illuminated by a TE-polarized plane wave: the narrow dark line indicates the BSW dispersion curve; (b) sketch of the experimental setup.

The experimental setup is depicted in Fig. 1(b). A TE-polarized collimated CW Nd:YAG laser beam ($\lambda = 532.0$ nm) illuminates the 1DPC oil-contacted to a glass prism according to the Kretschmann-Raether configuration. The prism is held on a motorized rotational stage allowing to accurately adjust the angle of incidence θ_e . The detection arm is mounted on an independent homocentric rotational stage, in such a way that the radiation leaving the sample with an angle θ_d , with respect to the normal to the sample, can be detected on either the prism or the air side of the 1DPC. Light is angularly filtered by two diaphragms (resulting in an angular acceptance of about 0.2°), spectrally filtered with an edge filter (RazorEdge from Semrock) for 532.0 nm radiation, and eventually focused into a fibered dispersive spectrometer (Ocean Optics USB2000+). Reference measurements obtained under the same conditions were also carried out using a bare glass substrate, on which a nominally identical PPAA layer grafted with fluorescent protein was deposited. We estimate the enhancement factor introduced by the 1DPC by comparing the fluorescence emission from both the multilayer and the glass slide.

Angularly resolved fluorescence spectra, obtained by exciting the samples at $\lambda = 532.0$ nm, are shown for the 1DPC and the glass slide in Figs. 2(a) and 2(b) and Figs. 2(c) and 2(d), respectively. Acquisition time was properly chosen in order to minimize the influence of dye photo bleaching during measurements.

In Figs. 2(a) and 2(c), directly emitted fluorescence spectra for 1DPC and glass are collected as a function of the exci-

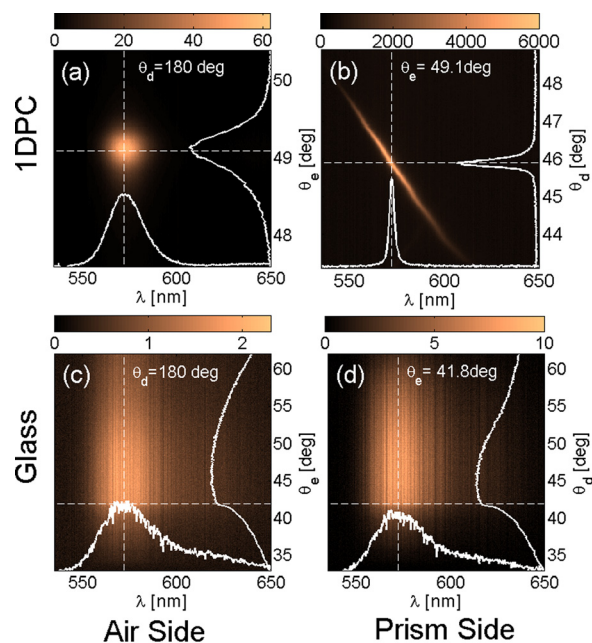


FIG. 2. (Color online) Fluorescence spectra (with background subtraction) for polymer-coated 1DPC (a) and (b) and glass (c) and (d) as a function of the laser excitation angle θ_e and detection angle θ_d (a), (c) and (b), (d), respectively. Angular and spectral profiles corresponding to relevant wavelengths or angles are also displayed (white solid lines). Intensities are after background subtraction and expressed in counts $\times 10^3$.

tation angle θ_e , while keeping the detection arm at normal position with respect to the sample. In Figs. 2(b) and 2(d), the excitation is kept fixed at the angle for which the fluorescence intensity is maximum, while the detection arm is collected the light that couples back and propagates into the prism.

In Fig. 2(a), a Lorentzian dependence for the 1DPC of the detected fluorescence on the illumination angle θ_e ($\Delta\theta_e \approx 0.4^\circ$) is observed. The maximum intensity is reached at the BSW resonance angle $\theta_e = 49.1^\circ$. When an angular scan is performed around this excitation angle with the detection arm, a strong dispersive behavior is observed (Fig. 2(b)), according to the BSW dispersion curve predicted in Fig. 1(a). This effect is due to the preferential coupling of the emitted fluorescence into BSW modes.^{13,14} As a consequence, a TE-polarized fluorescence signal is detected at those θ_d angles corresponding to almost monochromatic BSWs sustained by the 1DPC. In fact, because of the narrowness of BSW resonances, we observe that such a dispersive fluorescence emitted at different angles is in general spectrally narrow ($\Delta\lambda = 3$ nm) and with very low divergence ($\Delta\theta_d \approx 0.3^\circ$). In practice, since a measurement is the result of a convolution between the signal and the angular aperture of the collection optics ($\sim 0.2^\circ$), we infer that the actual spectral/angular width of the resonances is even smaller compared to the one actually measured. We compare this kind of results to those obtained from similar measurements on the glass slide. A weak angular dependence of the fluorescence intensity is found (Figs. 2(c) and 2(d)) and no modification of the emission spectrum at the air and prism side is observed. The observed peak width is indicative of the Q-factor of the associated mode. Because of the low intrinsic absorption of 1DPC, we expect the BSW-coupled fluorescence to show reduced spectral and angular widths as compared to a SPR-based configuration.

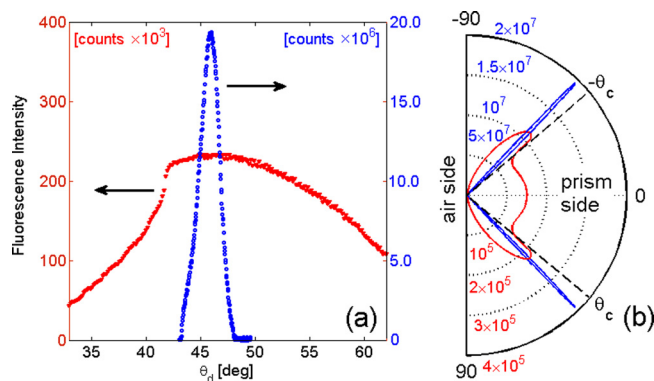


FIG. 3. (Color online) (a) Fluorescence intensity measured at the prism side: glass illuminated at $\theta_c = 41.8^\circ$ (triangles), 1DPC illuminated at $\theta_c = 49.1^\circ$ (squares); (b) Calculated angular distribution of the emitted radiation from an electric dipole on the surface of either a glass slide (broad angular distribution curve) or a 1DPC (narrow angular distribution curve). Intensities refer to an integral over the whole emission spectrum.

When the 1DPC is illuminated at $\theta_c = 49.1^\circ$, the near-field enhancement associated to the coupling of a laser BSW¹³ produces an enhanced fluorescence that is about 28 times larger than the fluorescence obtained from the glass slide illuminated at the critical angle $\theta_c = 41.8^\circ$ (Figs. 2(a) and 2(c)). A further improvement is obtained when the detection is performed at the prism-side, at those angles for which fluorescent BSWs are leaking out of the prism. For example, at $\theta_d = 46^\circ$, a further fluorescence enhancement of a factor of about 90 is observed (Fig. 2(b)), mainly caused by an angular/spectral redistribution of the radiated energy⁸ rather than an effective increase of the emitted power. For this last case, in order to avoid CCD saturation, a 0.25% transmission neutral filter was used. When compared to an analogous measurement on the glass slide, where both illumination and detection are performed at the critical angle, an overall detection enhancement of 560 is found (Fig. 2(d)).

The intrinsic dispersive nature of the BSW-coupled emission produces a spectral/angular distribution of the emitted power that is most useful in those applications where directionality, polarization, and spectral resolution are crucial, thus making multiplexing measurements feasible.¹⁵ However, for those applications where either or both spectral and angular resolution are not a concern, we show that there is still an advantage by using a BSW-based system. In Fig. 3(a), the fluorescence intensity is integrated over the whole spectrum and plotted as a function of the detection angle. A net two orders of magnitude improvement is still observed as compared to the case of a glass slide illuminated at the critical angle.

Experimental measurements are well supported by rigorous calculations based on a Green's function approach.¹⁶ We calculated the fluorescence intensities considering an electric dipole on both glass and 1DPC substrates with the polymeric layer. The dipole is oriented parallel to the sample surface and therefore can be excited by TE-polarized light. The illumination conditions considered in the calculations match those used in the experiment. A pictorial view of the angular distribution of the power radiated into the prism is presented in Fig. 3(b). Two narrow angular lobes peaked in the region of the BSW dispersion curve show the enhanced emission, as confirmed by the measurements.

Although the underlying physics is rather different, the presented BSW-controlled emission can be exploited as an alternative to SPCE and SPFS in biosensing applications, leading to analogous or even improved effects. In a previous work,¹⁴ directional coupling from a rhodamine monolayer through BSWs has been demonstrated, leading to an improvement factor of about one order of magnitude. In the present work, by taking advantage of both BSW-driven illumination and emission, we observed an enhancement factor of about 560 on the detected fluorescence in a similar configuration. The use of all-dielectric 1DPC structures presents clear advantages associated to low or almost zero absorption, narrow BSW resonances, spectral and polarization tunability, and low intrinsic chemical reactivity of the materials employed. Opposite to the case of plasmons on metal films, when designing a 1DPC aimed at a given sensing application, it is possible to explicitly take into account and thus compensate the presence of a functionalization/tailoring layer (such as a 30 nm thick PPAA layer, as used herein). In such a way, the emitters (not only organic dyes, but Q-dots as well¹⁷) can always be located at a suitable distance to the structure in order to optimize the radiated power after coupling to the BSW modes. If a functional/tailoring layer is surface patterned, complex emitting structures for guiding BSW can be obtained.^{18–20}

The authors acknowledge very useful discussions with N. Danz, Fraunhofer IOF, Jena. This work is supported by the Piedmont Regional project CIPE 2008 "PHotonic bio-sensors for Early caNcer diagnosticS (PHOENICS)."

¹J. R. Lakowicz, *Principles of Fluorescence Spectroscopy*, 3rd ed. (Springer; New York, 2006).

²T. Liebermann and W. Knoll, *Colloids Surf., A* **171**, 115 (2000).

³J. R. Lakowicz, K. Ray, M. Chowdhury, H. Szmajcinski, Y. Fu, J. Zhang, and K. Nowaczyk, *Analyst* **133**, 1308 (2008).

⁴J. Dostalek and W. Knoll, *BioInterphases* **3**, 12 (2008).

⁵I. Gryczynski, J. Malicka, Z. Gryczynski, and J. R. Lakowicz, *Anal. Biochem.* **324**, 170 (2004).

⁶N. Calander, *Anal. Chem.* **76**, 2168 (2004).

⁷R. S. Satish, Y. Kostov, and G. Rao, *Appl. Phys. Lett.* **94**, 223113 (2009).

⁸J. Enderlein and T. Ruchstuhl, *Opt. Express* **13**, 8855 (2005).

⁹K. Ray, H. Szmajcinski, J. Enderlein, and J. R. Lakowicz, *Appl. Phys. Lett.* **90**, 251116 (2007).

¹⁰Y. Guo, J. Y. Ye, C. Divin, B. Huang, T. P. Thomas, J. R. Baker, Jr., and T. B. Norris, *Anal. Chem.* **82**, 5211 (2010).

¹¹F. Michelotti, B. Sciacca, L. Dominici, M. Quaglio, E. Descrovi, F. Giorgis, and F. Geobaldo, *Phys. Chem. Chem. Phys.* **12**, 502 (2010).

¹²S. Ricciardi, R. Castagna, S. M. Severino, I. Ferrante, F. Frascella, E. Celasco, P. Mandracci, I. Vallini, G. Mantero, C.F. Pirri, and P. Rivolo, *Plasma Processes Polym.* (submitted).

¹³I. V. Soboleva, E. Descrovi, C. Summonte, A. A. Fedyanin, and F. Giorgis, *Appl. Phys. Lett.* **94**, 231122 (2009).

¹⁴M. Liscidini, M. Galli, M. Shi, G. Dacarro, M. Patrini, D. Bajoni, and J. E. Sipe, *Opt. Lett.* **34**, 2318 (2009).

¹⁵E. Matveeva, J. Malicka, I. Gryczynski, Z. Gryczynski, and J. R. Lakowicz, *Biochem. Biophys. Res. Commun.* **313**, 721 (2004).

¹⁶N. Danz, R. Waldhaeusl, A. Braeuer, and R. Kowarschik, *J. Opt. Soc. Am. A* **19**, 412 (2002).

¹⁷I. Gryczynski, J. Malicka, W. Jiang, H. Fischer, W. C. W. Chan, Z. Gryczynski, W. Grudzinski, and J. R. Lakowicz, *J. Phys. Chem. B* **109**, 1088 (2005).

¹⁸E. Descrovi, F. Giorgis, L. Dominici, and F. Michelotti, *Opt. Lett.* **33**, 243 (2008).

¹⁹E. Descrovi, T. Sfez, M. Quaglio, D. Brunazzo, L. Dominici, F. Michelotti, H. P. Herzig, O. J. F. Martin, and F. Giorgis, *Nano Lett.* **10**, 2087 (2010).

²⁰M. Liscidini, D. Gerace, D. Sanvitto, and D. Bajoni, *Appl. Phys. Lett.* **98**, 121118 (2011).